

5

Nonlinear integrate-and-fire models

Detailed conductance-based neuron models can reproduce electrophysiological measurements to a high degree of accuracy, but because of their intrinsic complexity these models are difficult to analyze. For this reason, simple phenomenological spiking neuron models are highly popular for studies of neural coding, memory, and network dynamics. In this chapter we discuss formal threshold models of neuronal firing, also called integrate-and-fire models.

The shape of the action potential of a given neuron is rather stereotyped with very little change between one spike and the next. Thus, the shape of the action potential which travels along the axon to a postsynaptic neuron cannot be used to transmit information; rather, from the point of view of the receiving neuron, action potentials are “events” which are fully characterized by the arrival time of the spike at the synapse. Note that spikes from different neuron types can have different shapes and the duration and shape of the spike does influence neurotransmitter release; but the spikes that arrive at a given synapse all come from the same presynaptic neuron and – if we neglect effects of fatigue of ionic channels in the axon – we can assume that its time course is always the same. Therefore we make no effort to model the exact shape of an action potential. Rather, spikes are treated as events characterized by their firing time – and the task consists in finding a model so as to reliably predict spike timings.

In generalized integrate-and-fire models, spikes are generated whenever the membrane potential u crosses some threshold θ_{reset} from below. The moment of threshold crossing defines the firing time t^f ,

$$t^f : \quad u(t^f) = \theta_{\text{reset}} \quad \text{and} \quad \left. \frac{du(t)}{dt} \right|_{t=t^f} > 0. \quad (5.1)$$

In contrast to the two-dimensional neuron models, encountered in Chapter 4, we don’t have a relaxation variable that enables us to describe the return of the membrane potential to rest. In the integrate-and-fire models, discussed in this and the following chapters, the downswing of the action potential is replaced by an algorithmic reset of the membrane potential to a new value u_r each time the threshold θ_{reset} is reached. The duration of an action potential is sometimes, but not always, replaced by a dead-time Δ^{abs} after each spike, before the voltage dynamics restarts with $u = u_r$ as initial condition.

In this chapter, we focus on integrate-and-fire models with a single variable u which describes the time course of the membrane potential. In Chapter 6, we extend the models developed in this chapter so as to include adaptation of neuronal firing during extended strong stimulation. In Chapters 7–11 we consider questions of coding, noise, and reliability of spike-time prediction – using the generalized integrate-and-fire model which we introduce now.

5.1 Thresholds in a nonlinear integrate-and-fire model

In a general *nonlinear* integrate-and-fire model with a single variable u , the membrane potential evolves according to

$$\tau \frac{d}{dt} u = f(u) + R(u)I. \quad (5.2)$$

As mentioned above, the dynamics is stopped if u reaches the threshold θ_{reset} . In this case the firing time t^f is noted and integration of the membrane potential equation restarts at time $t^f + \Delta^{\text{abs}}$ with initial condition u_r . A typical example of the function $f(u)$ in Eq. (5.2) is shown in Fig. 5.1. If not specified otherwise, we always assume in the following a constant input resistance $R(u) = R$ independent of voltage.

A comparison of Eq. (5.2) with the equation of the standard leaky integrate-and-fire model

$$\tau \frac{d}{dt} u = -(u - u_{\text{rest}}) + RI, \quad (5.3)$$

which we encountered in Chapter 1, shows that the nonlinear function $R(u)$ can be interpreted as a voltage-dependent input resistance while $f(u)$ replaces the leak term $-(u - u_{\text{rest}})$. Some well-known examples of nonlinear integrate-and-fire models include the exponential integrate-and-fire model (Section 5.2) and the quadratic integrate-and-fire model (Section 5.3). Before we turn to these specific models, we discuss some general aspects of nonlinear integrate-and-fire models.

Example: Rescaling and standard forms (*)

It is always possible to rescale the variables in Eq. (5.2) so that the threshold and membrane time constant are equal to unity and the resting potential vanishes. Furthermore, there is no need to interpret the variable u as the membrane potential. For example, starting from the nonlinear integrate-and-fire model Eq. (5.2), we can introduce a new variable \tilde{u} by the transformation

$$u(t) \longrightarrow \tilde{u}(t) = \tau \int_0^{u(t)} \frac{dx}{R(x)}, \quad (5.4)$$

which is possible if $R(x) \neq 0$ for all x in the integration range. In terms of \tilde{u} we have a

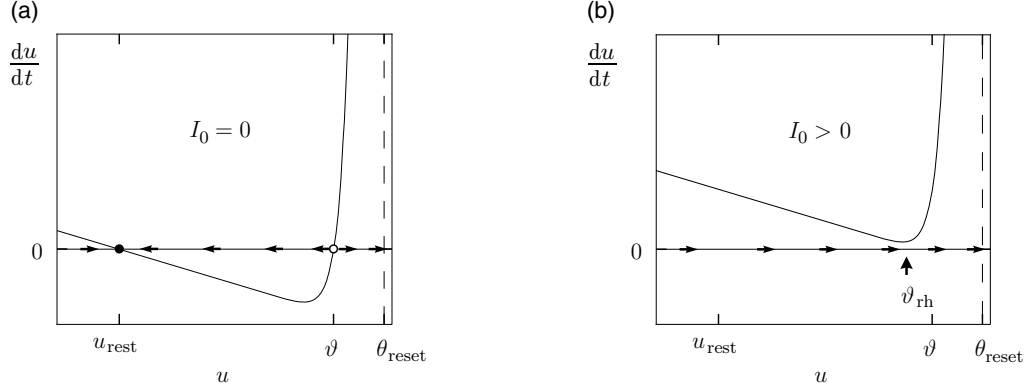


Fig. 5.1 Thresholds in a nonlinear integrate-and-fire model. The change du/dt of the voltage is plotted as a function $f(u)$ of the voltage u . (a) In the absence of stimulation $I_0 = 0$, the zero-crossings $du/dt = 0$ define the resting potential u_{rest} and the firing threshold ϑ of the nonlinear integrate-and-fire model. A positive change in the membrane potential $du/dt = f(u) > 0$ implies that the voltage increases (flow arrow to the right), while $du/dt < 0$ implies a decay of the voltage. The pattern of arrows indicates a stable fixed point at rest, but an unstable fixed point at ϑ . Whenever the voltage reaches the value θ_{reset} the voltage is reset to a lower value. (b) For a constant positive input $I_0 > 0$, the curve of du/dt is shifted vertically upward. The rheobase threshold ϑ_{rh} indicates the maximal voltage that can be reached with constant current injection before the neuron starts repetitive firing.

new nonlinear integrate-and-fire model of the form

$$\frac{d\tilde{u}}{dt} = d(\tilde{u}) + I(t) \quad (5.5)$$

with $d(\tilde{u}) = f(u)/R(u)$. In other words, a general integrate-and-fire model (5.2) can always be reduced to the standard form (5.5). By a completely analogous transformation, we could eliminate the voltage-dependence of the function f in Eq. (5.2) and move all the dependence into a new voltage-dependent $R(u)$ (Abbott and van Vreeswijk, 1993).

5.1.1 Where is the firing threshold?

In the standard leaky integrate-and-fire model, the linear equation Eq. (5.3) is combined with a numerical threshold θ_{reset} . We may interpret θ_{reset} as the firing threshold in the sense of the minimal voltage necessary to cause a spike, whatever stimulus we choose. In other words, if the voltage is currently marginally below θ_{reset} and no further stimulus is applied, the neuron inevitably returns to rest. If the voltage reaches θ_{reset} , the neuron fires. For nonlinear integrate-and-fire models, such a clear-cut picture of a firing threshold no longer holds.

The typical shape of a function $f(u)$ used in the nonlinear integrate-and-fire model defined in Eq. (5.2) is sketched in Fig. 5.1. Around the resting potential, the function f is linear and proportional to $(u - u_{\text{rest}})$. But in contrast to the leaky integrate-and-fire model

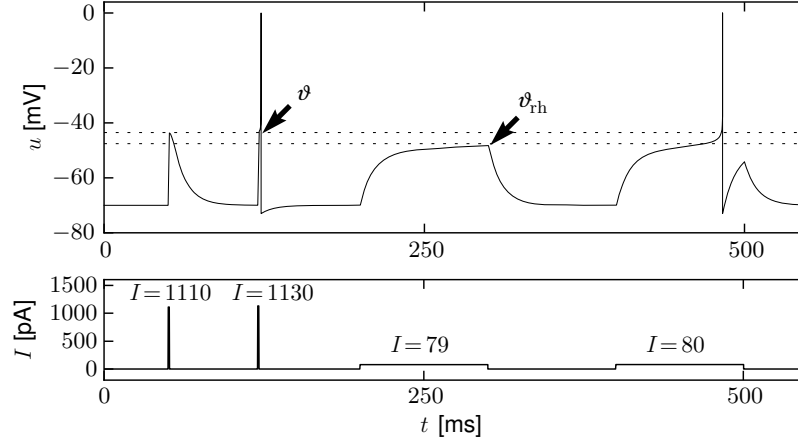


Fig. 5.2 Stimulation of a nonlinear integrate-and-fire model with pulses and step currents. Voltage as a function of time (top) in response to the currents indicated at the bottom. The firing threshold ϑ found with pulse stimuli and the threshold ϑ_{rh} for repetitive firing under prolonged current injection are indicated by the dashed horizontal lines.

of Eq. (5.3) where the voltage dependence is linear everywhere, the function $f(u)$ of the nonlinear model turns at some point sharply upwards.

If the nonlinear integrate-and-fire model is stimulated with currents of various shapes, we can identify, from the simulation of the model, the threshold for spike generation. We search for the maximal voltage which can be reached before the model fires a spike. Figure 5.2 shows that the voltage threshold ϑ determined with pulse-like input currents is different from the voltage threshold determined with prolonged step currents.

For an explanation, we return to Fig. 5.1a which shows du/dt as a function of u . There are two zero-crossings $du/dt = f(u) = 0$, which we denote as u_{rest} and ϑ , respectively. The first one, u_{rest} , is a stable fixed point of the dynamics, whereas ϑ is an unstable one.

A short current pulse $I(t) = q\delta(t - t_0)$ injected into Eq. (5.2) delivers at time t_0 a total charge q and causes a voltage step of size $\Delta u = Rq/\tau$ (see Section 1.3.2). The new voltage $u = u_{rest} + \Delta u$ serves as initial condition for the integration of the differential equation *after* the input pulse. For $u < \vartheta$ the membrane potential returns to the resting potential, while for $u > \vartheta$ the membrane potential increases further, until the increase is stopped at the numerical threshold θ_{reset} . Thus the unstable fixed point ϑ serves as a voltage threshold, if the neuron model is stimulated by a short current pulse.

Under the application of a constant current, the picture is different (Fig. 5.1b). Since we plot du/dt along the vertical axis, a constant current I_0 shifts the curve of du/dt shown in Fig. 5.1a vertically upward to a new value $f(u) + RI_0$; see Eq. (5.2). If the current is sufficiently large, both fixed points disappear so that du/dt is always positive. As a result, the voltage increases until it hits the numerical threshold θ_{reset} , at which point it is reset and the same picture repeats. In other words, the neuron model has entered the regime of repetitive firing.

The critical current for initiation of repetitive firing corresponds to the voltage where the stable fixed point disappears, or $\vartheta_{\text{rh}} = I_c R$. In the experimental literature, the critical current $I_c = \vartheta_{\text{rh}}/R$ is called the “rheobase” current. In the mathematical literature, it is called the bifurcation point. Note that a stationary voltage $u > \vartheta_{\text{rh}}$ is not possible. On the other hand, for pulse inputs or time-dependent currents, voltage transients into the regime $\vartheta_{\text{rh}} < u(t) < \vartheta$ routinely occur without initiating a spike.

5.1.2 Detour: Analysis of one-dimensional differential equations

For those readers who are not familiar with figures such as Fig. 5.1, we add a few mathematical details.

The momentary state of one-dimensional differential equations such as Eq. (5.2) is completely described by a single variable, called u in our case. This variable is plotted in Fig. 5.1 along the horizontal axis. An increase in voltage corresponds to a movement to the right, a decrease to a movement to the left. Thus, in contrast to the phase plane analysis of two-dimensional neuron models, encountered in Section 4.3, the momentary state of the system always lies on the horizontal axis.

Let us suppose that the momentary value of the voltage is $u(t_0)$. The value a short time afterwards is given by $u(t_0 + \Delta t) = u(t_0) + \dot{u} \Delta t$ where $\dot{u} = du/dt$ is given by the differential equation Eq. (5.2). The difference $u(t_0 + \Delta t) - u(t_0)$ is positive if $\dot{u} > 0$ and indicated by a flow arrow to the right; the arrow points leftwards if $\dot{u} < 0$.

A nice aspect of a plot such as in Fig. 5.1a is that, for each u , the vertical axis of the plot indicates $\dot{u} = f(u)$, i.e., we can directly read off the value of the flow without further calculation. If the value of the function $f(u)$ is above zero, the flow is to the right; if it is negative, the flow is to the left.

By definition, the flow du/dt vanishes at the fixed points. Thus fixed points are given by the zero-crossings $f(u) = 0$ of the curve. Moreover, the flow pattern directly indicates the stability of a fixed point. From the figure, we can read off that a fixed point at u_0 is stable (arrows pointing towards the fixed point) if the slope of the curve df/du evaluated at u_0 is negative.

The mathematical proof goes as follows. Suppose that the system is, at time t_0 , slightly perturbed around the fixed point to a new value $u_0 + x(t_0)$. We focus on the evolution of the perturbation $x(t)$. The perturbation follows the differential equation $dx/dt = \dot{u} = f(u_0 + x)$. Taylor expansion of f around u_0 gives $dx/dt = f(u_0) + (df/du)_{u_0} x$. At the fixed point, $f(u_0) = 0$. The solution of the differential equation therefore is $x(t) = x(t_0) \exp[b(t - t_0)]$. If the slope $b = (df/du)_{u_0}$ is negative, the amplitude of the perturbation $x(t)$ decays back to zero, indicating stability. Therefore, negative slope $(df/du)_{u_0} < 0$ implies stability of the fixed point.

5.2 Exponential integrate-and-fire model

In the exponential integrate-and-fire model (Fourcaud-Trocme *et al.*, 2003), the differential equation for the membrane potential is given by

$$\tau \frac{d}{dt} u = -(u - u_{\text{rest}}) + \Delta_T \exp\left(\frac{u - \vartheta_{\text{rh}}}{\Delta_T}\right) + RI. \quad (5.6)$$

The first term on the right-hand side of Eq. (5.6) is identical to Eq. (5.3) and describes the leak of a passive membrane. The second term is an exponential nonlinearity with “sharpness” parameter Δ_T and “threshold” ϑ_{rh} .

The moment when the membrane potential reaches the numerical threshold θ_{reset} defines the firing time t^f . After firing, the membrane potential is reset to u_r and integration restarts at time $t^f + \Delta^{\text{abs}}$ where Δ^{abs} is an absolute refractory time, typically chosen in the range $0 < \Delta^{\text{abs}} < 5$ ms. If the numerical threshold is chosen sufficiently high, $\theta_{\text{reset}} \gg \vartheta + \Delta_T$, its exact value does not play any role. The reason is that the upswing of the action potential for $u \gg \vartheta + \Delta_T$ is so rapid that it goes to infinity in an incredibly short time (Touboul, 2009). The threshold θ_{reset} is introduced mainly for numerical convenience. For a formal mathematical analysis of the model, the threshold can be pushed to infinity.

Example: Rheobase threshold and interpretation of parameters

The exponential integrate-and-fire model is a special case of the general nonlinear model defined in Eq. (5.2) with a function

$$f(u) = -(u - u_{\text{rest}}) + \Delta_T \exp\left(\frac{u - \vartheta_{\text{rh}}}{\Delta_T}\right). \quad (5.7)$$

In the absence of external input ($I = 0$), the differential equation of the exponential integrate-and-fire model (5.6) has two fixed points, defined by the zero-crossings $f(u) = 0$; see Fig. 5.1a. We suppose that parameters are chosen such that $\vartheta_{\text{rh}} \gg u_{\text{rest}} + \Delta_T$. Then the stable fixed point is at $u \approx u_{\text{rest}}$ because the exponential term becomes negligibly small for $u \ll \vartheta_{\text{rh}} - \Delta_T$. The unstable fixed point which acts as a threshold for pulse input lies to the right-hand side of ϑ_{rh} .

If the external input increases slowly in a quasi-constant fashion, the two fixed points move closer together until they finally merge at the bifurcation point; see Fig. 5.1b. The voltage at the bifurcation point can be determined from the condition $df/du = 0$ to lie at $u = \vartheta_{\text{rh}}$. Thus ϑ_{rh} is the threshold found with constant (rheobase) current, which justifies its name.

Example: Relation to the leaky integrate-and-fire model

In the exponential integrate-and-fire model, the voltage threshold ϑ for pulse input is different from the rheobase threshold ϑ_{rh} for constant input (Fig. 5.1). However, in the limit $\Delta_T \rightarrow 0$, the sharpness of the exponential term increases and ϑ approaches ϑ_{rh} .

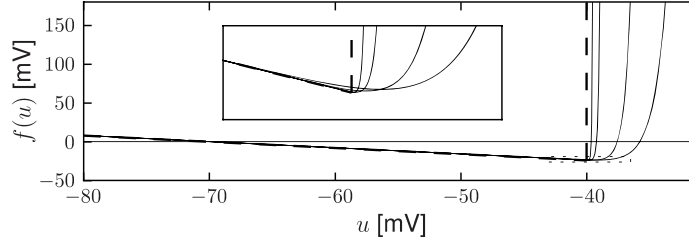


Fig. 5.3 Exponential and leaky integrate-and-fire model. The function $f(u)$ is plotted for different choices of the “sharpness” of the threshold ($\Delta_T = 1, 0.5, 0.25, 0.05$ mV). In the limit $\Delta_T \rightarrow 0$ the exponential integrate-and-fire model becomes equivalent to a leaky integrate-and-fire model (dashed line). The inset shows a zoom onto the threshold region (dotted box).

(Fig. 5.3). In the limit, $\Delta_T \rightarrow 0$, we can approximate the nonlinear function by the linear term

$$f(u) = -(u - u_{\text{rest}}) \quad \text{for } u < \vartheta_{\text{th}} \quad (5.8)$$

and the model fires whenever u reaches $\vartheta_{\text{th}} = \vartheta$. Thus, in the limit $\Delta_T \rightarrow 0$, we return to the leaky integrate-and-fire model.

5.2.1 Extracting the nonlinearity from data

Why should we choose an exponential nonlinearity rather than any other nonlinear dependence in the function $f(u)$ of the general nonlinear integrate-and-fire model? Can we use experimental data to determine the “correct” shape of $f(u)$ in Eq. (5.2)?

We can rewrite the differential equation (5.2) of the nonlinear integrate-and-fire model by moving the function $f(u)$ to the left-hand side and all other terms to the right-hand-side of the equation. After rescaling with the time constant τ , the nonlinearity $\tilde{f}(u) = f(u)/\tau$ is

$$\tilde{f}(u(t)) = \frac{1}{C} I(t) - \frac{d}{dt} u(t), \quad (5.9)$$

where $C = \tau/R$ can be interpreted as the capacity of the membrane.

In order to determine the function $\tilde{f}(u)$, an experimenter injects a time-dependent current $I(t)$ into the soma of a neuron while measuring with a second electrode the voltage $u(t)$. From the voltage time course, one finds the voltage derivative du/dt .

A measurement at time t yields a value $u(t)$ (which we use as value along the x -axis of a plot) and a value $[(I(t)/C) - (du/dt)]$ (which we plot along the y -axis). With a thousand or more time points per second, the plot fills up rapidly. For each voltage u there are many data points with different values along the y -axis. The best choice of the parameter C is the one that minimizes the width of this distribution. At the end, we average across all points at a given voltage u to find the empirical function (Badel *et al.*, 2008a)

$$\tilde{f}(u(t)) = \left\langle \frac{1}{C} I(t) - \frac{d}{dt} u(t) \right\rangle, \quad (5.10)$$

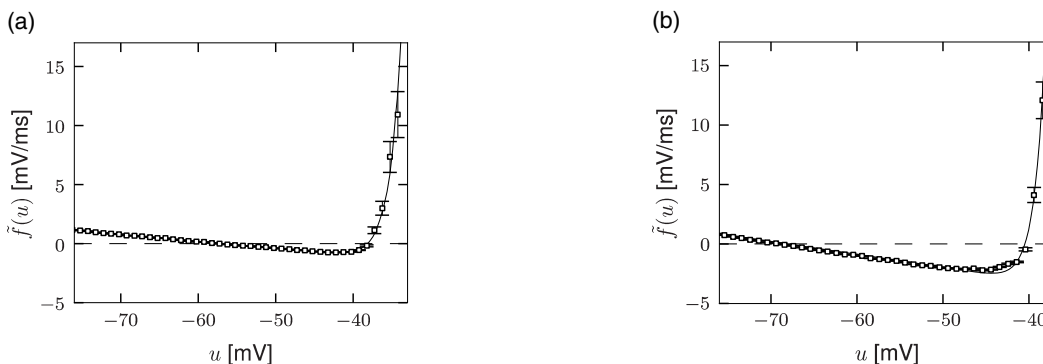


Fig. 5.4 Extracting nonlinear integrate-and-fire models from data. The function $f(u)$ characterizing the nonlinearity of an integrate-and-fire model according to Eq. (5.2) is derived from experimental data using random current injection into neurons. (a) Cortical pyramidal cells. Experimental data points (symbols) and fit by an exponential integrate-and-fire model. (b) As in (a), but for an inhibitory interneuron. Data courtesy of Laurent Badel and Sandrine Lefort (Badel *et al.*, 2008a).

where the angle brackets indicate averaging. This function is plotted in Fig. 5.4. We find that the empirical function extracted from experiments is well approximated by a combination of a linear and exponential term

$$\tilde{f}(u) = -\frac{u - u_{\text{rest}}}{\tau} + \frac{\Delta_T}{\tau} \exp\left(\frac{u - \vartheta_{\text{rh}}}{\Delta_T}\right), \quad (5.11)$$

which provides an empirical justification of the choice of nonlinearity in the exponential integrate-and-fire model.

We note that the slope of the curve at the resting potential is related to the membrane time constant τ while the threshold parameter ϑ_{rh} is the voltage at which the function \tilde{f} goes through its minimum.

Example: Refractory exponential integrate-and-fire model

The above procedure for determining the nonlinearity can be repeated for a set of data points restricted to a few milliseconds *after* an action potential (Fig. 5.6). After a spike, the threshold ϑ_{rh} is slightly higher, which is one of the signs of refractoriness. Moreover, the location of the zero-crossing u_{rest} and the slope of the function \tilde{f} at u_{rest} are different, which is to be expected since after a spike the sodium channel is inactivated while several other ion channels are open. All parameters return to the “normal” values within a few tens of milliseconds. An exponential integrate-and-fire model where the parameters depend on the time since the last spike has been called the “refractory exponential integrate-and-fire model” (Badel *et al.*, 2008a). The refractory exponential integrate-and-fire model predicts the voltage time course of a real neuron for novel time-dependent stimuli to a high degree of accuracy, if the input statistics is similar to the one used for parameter extraction (Fig. 5.5).

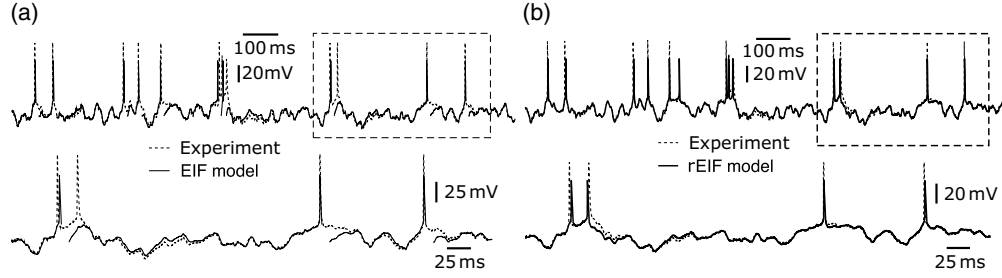


Fig. 5.5 Predicting the membrane voltage with an exponential integrate-and-fire model. (a) Comparison of membrane voltage in experiments (thick line) with the predictions of the exponential integrate-and-fire model (thin line). The fit is excellent, except during a short period after a spike. (b) Same as in (a), but in a model with refractoriness. Modified from Badel *et al.* (2008b).

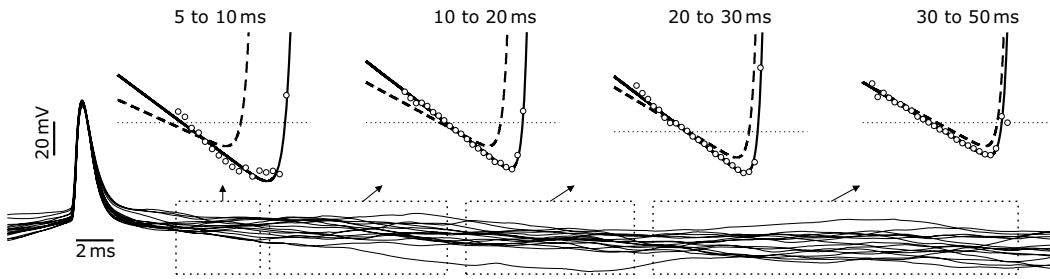


Fig. 5.6 Refractory effects in the exponential integrate-and-fire model. Top: Because of refractoriness immediately after a spike, the exponential integrate-and-fire model has a higher firing threshold and increased slope in the linear section. Data points and fit as in Fig. 5.4, but data points restricted to intervals 5–10 ms (far left), 10–20 ms (left), 20–30 ms (right), or 30–50 ms (far right) after a spike. As the time since the last spike increases, refractoriness decays and the parameters of the exponential integrate-and-fire model approach their standard values (dashed lines). Bottom: Sample voltage traces during and after a spike. From Badel *et al.* (2008b).

5.2.2 From Hodgkin–Huxley to exponential integrate-and-fire

In Section 4.2 we have already seen that the four-dimensional system of equations of Hodgkin and Huxley can be reduced to two equations. Here we show how to take a further step so as to arrive at a single nonlinear differential equation combined with a reset (Jolivet *et al.*, 2004).

After appropriate rescaling of all variables, the system of two equations that summarizes a Hodgkin–Huxley model reduced to two dimensions can be written as

$$\frac{du}{dt} = F(u, w) + I, \quad (5.12)$$

$$\frac{dw}{dt} = \varepsilon G(u, w), \quad (5.13)$$

which is just a copy of Eqs. (4.33) and (4.34) in Section 4.6; note that time is measured in units of the membrane time constant τ_m and that the resistance has been absorbed into

the definition of the current I . The function $F(u, w)$ is given by Eqs. (4.3) and (4.4). The exact shape of the function $G(u, w)$ has been derived in Section 4.2, but plays no role in the following. We recall that the fixed points are defined by the condition $du/dt = dw/dt = 0$. For the case without stimulation $I = 0$, we denote the variables at the *stable* fixed point as u_{rest} (resting potential) and w_{rest} (resting value of the second variable).

In the following we assume that there is a separation of time scales ($\varepsilon \ll 1$) so that the evolution of the variable w is much slower than that of the voltage. As discussed in Section 4.6, this implies that all flow arrows in the two-dimensional phase plane are horizontal except those in the neighborhood of the u -nullcline. In particular, after a stimulation with short current pulses, the trajectories move horizontally back to the resting state (no spike elicited) or horizontally leftward (upswing of an action potential) until they hit one of the branches of the u -nullcline; see Fig. 4.22. In other words, the second variable stays at its resting value $w = w_{\text{rest}}$ and can therefore be eliminated – unless we want to describe the exact shape of the action potential. As long as we are only interested in the initiation phase of the action potential we can assume a fixed value $w = w_{\text{rest}}$.

For constant w , Eq. (5.12) becomes

$$\frac{du}{dt} = F(u, w_{\text{rest}}) + I = f(u) + I, \quad (5.14)$$

which has the form of a nonlinear integrate-and-fire neuron. The resulting function $f(u)$ is plotted in Fig. 5.7a. It has three zero-crossings: the first one (left) at u_{rest} , corresponding to a stable fixed point; a second one (middle) which acts as a threshold ϑ ; and a third one to the right, which is again a stable fixed point and limits the upswing of the action potential. The value of the reset threshold $\theta_{\text{reset}} > \vartheta$ should be reached during the upswing of the spike and must therefore be chosen between the second and third fixed point. While in the two-dimensional model the variable w is necessary to describe the downswing of the action potential on a smooth trajectory back to rest, we replace the downswing in the nonlinear integrate-and-fire model by an artificial reset of the voltage variable to a value u_r whenever u hits θ_{reset} .

If we focus on the region $u < \theta_{\text{reset}}$, the function $f(u) = F(u, w_{\text{rest}})$ is very well approximated by the nonlinearity of the exponential integrate-and-fire model (Fig. 5.7b).

Example: Exponential activation of sodium channels

In the previous section, we followed a series of formal mathematical steps, from the two-dimensional version of the Hodgkin–Huxley model to a one-dimensional differential equation which looked like a combination of linear and exponential terms, i.e., an exponential integrate-and-fire model. For a more biophysical derivation and interpretation of the exponential integrate-and-fire model, it is, however, illustrative to start directly with the voltage equation of the Hodgkin–Huxley model, (2.4)–(2.5), and replace the variables h and n by their values at rest, h_{rest} and n_{rest} , respectively. Furthermore, we assume that m approaches instantaneously its equilibrium value $m_0(u)$.

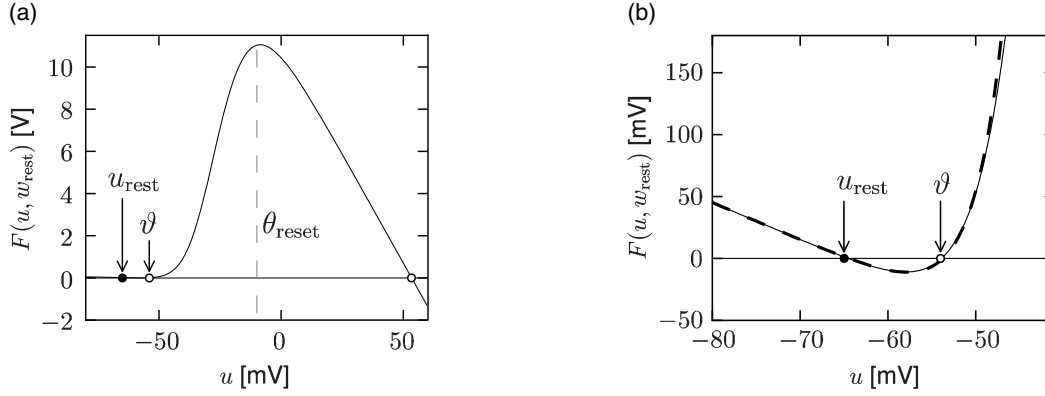


Fig. 5.7 Approximating Hodgkin–Huxley by an exponential integrate-and-fire model. (a) The value of the $F(u, w_{\text{rest}})$ for fixed value of the second variable $w = w_{\text{rest}}$ is plotted as a function of the voltage variable u . The choice of a reset threshold θ_{reset} is indicated. (b) Solid line as in A, restricted to $u < \theta_{\text{reset}}$. The dashed line shows the approximation by an exponential integrate-and-fire model.

This yields

$$C \frac{du}{dt} = -g_{\text{Na}} [m_0(u)]^3 h_{\text{rest}} (u - E_{\text{Na}}) - g_{\text{K}} (n_{\text{rest}})^4 (u - E_{\text{K}}) - g_{\text{L}} (u - E_{\text{L}}) + I. \quad (5.15)$$

Potassium and leak currents can now be summed up to a new effective leak term $g^{\text{eff}}(u - E^{\text{eff}})$. In the voltage range close to the resting potential the driving force $(u - E_{\text{Na}})$ of the sodium current can be well approximated by $(u_{\text{rest}} - E_{\text{Na}})$. Then the only remaining nonlinearity on the right-hand side of Eq. (5.15) arises from $m_0(u)$. For voltages around rest, $m_0(u)$ has, however, an exponential shape. In summary, the right-hand side of Eq. (5.15) can be approximated by a linear and an exponential term – and this gives rise to the exponential integrate-and-fire model (Fourcaud-Trocme *et al.*, 2003).

5.3 Quadratic integrate and fire

A specific instance of a nonlinear integrate-and-fire model is the *quadratic* model (Latham *et al.*, 2000; Hansel and Mato, 2001),

$$\tau \frac{d}{dt} u = a_0 (u - u_{\text{rest}}) (u - u_c) + RI, \quad (5.16)$$

with parameters $a_0 > 0$ and $u_c > u_{\text{rest}}$; see Fig. 5.8a. For $I = 0$ and initial condition $u < u_c$, the voltage decays to the resting potential u_{rest} . For $u > u_c$ it increases so that an action potential is triggered. The parameter u_c can therefore be interpreted as the critical voltage for spike initiation by a short current pulse. We will see in the next subsection that the quadratic integrate-and-fire model is closely related to the so-called Θ -neuron, a canonical type-I neuron model (Ermentrout, 1996; Latham *et al.*, 2000).

For numerical implementation of the model, the integration of Eq. (5.16) is stopped if the voltage reaches a numerical threshold θ_{reset} and restarted with a reset value u_r as

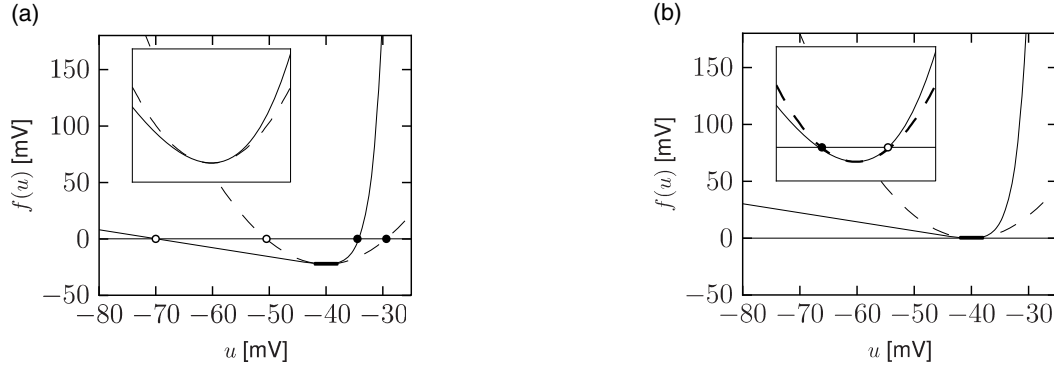


Fig. 5.8 Quadratic integrate-and-fire model. (a) The quadratic integrate-and-fire model (dashed line), compared with an exponential integrate-and-fire model (solid line). (b) The quadratic integrate-and-fire model can be seen as an approximation of an exponential integrate-and-fire model (or any other type I model) depolarized to a state close to repetitive firing. In (a) and (b), the value $f(u)$ and curvature d^2f/du^2 are matched at $u = v_{th}$. Note that the rise in the quadratic model is slower in the superthreshold regime $u > v_{th}$.

new initial condition (Fig. 5.9b). For a mathematical analysis of the model, however, the standard assumption is $\theta_{reset} \rightarrow \infty$ and $u_r \rightarrow -\infty$.

We have seen in the previous section that experimental data suggests an exponential, rather than quadratic nonlinearity. However, close to the threshold for repetitive firing, the exponential integrate-and-fire model and the quadratic integrate-and-fire model become very similar (Fig. 5.8b). Therefore the question arises whether the choice between the two models is a matter of personal preference only.

For a mathematical analysis, the quadratic integrate-and-fire model is sometimes more handy than the exponential one. However, the fit to experimental data is much better with the exponential than with the quadratic integrate-and-fire model. For a prediction of spike times and voltage of real neurons (see Fig. 5.5), it is therefore advisable to work with the exponential rather than the quadratic integrate-and-fire model. Loosely speaking, the quadratic model is too nonlinear in the subthreshold regime and the upswing of a spike is not rapid enough once the voltage is above threshold. The approximation of the exponential integrate-and-fire model by a quadratic one only holds if the mean driving current is close to the rheobase current.

Example: Approximating the exponential integrate-and-fire

Let us suppose that an exponential integrate-and-fire model is driven by a depolarizing current that shifts its effective equilibrium potential u_r^{eff} close to the rheobase firing threshold v_{th} . The stable fixed points at $u = u_r^{eff}$ and the unstable fixed point at $u = v_{th}^{eff}$ corresponding to the effective firing threshold for pulse injection now lie symmetrically around v_{th} (Fig. 5.8b). In this region, the shape of the function $f(u)$ is well approximated

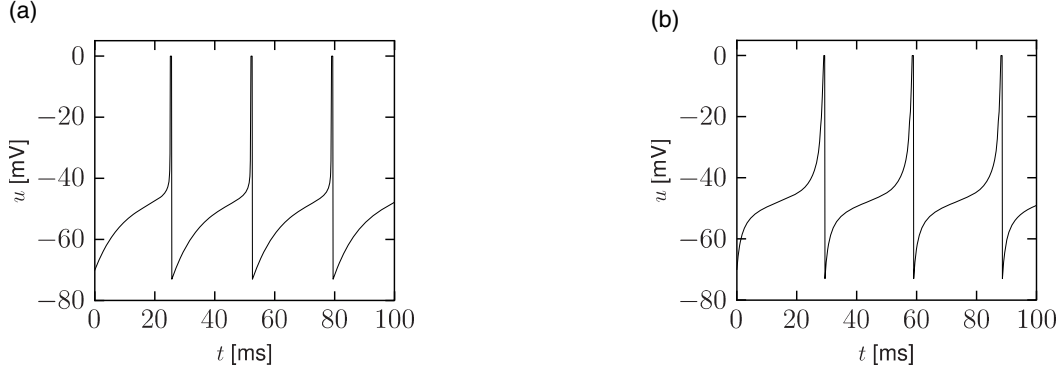


Fig. 5.9 Repetitive firing in nonlinear integrate-and-fire models. (a) Exponential integrate-and-fire model and (b) quadratic integrate-and-fire model receiving a constant current sufficient to elicit repetitive firing. Note the comparatively slow upswing of the action potential in the quadratic integrate-and-fire model. Numerical simulation with parameters of equivalent models as illustrated in Fig. 5.8.

by a quadratic function (dashed line). In other words, in this regime the exponential and quadratic integrate-and-fire neuron become identical.

If the constant input current is increased further, the stable and unstable fixed point move closer together and finally merge and disappear at the bifurcation point, corresponding to a critical current I_c . More generally, any type I neuron model close to the bifurcation point can be approximated by a quadratic integrate-and-fire model – and this is why it is sometimes called the “canonical” type I integrate-and-fire model (Ermentrout, 1996; Ermentrout and Kopell, 1986).

5.3.1 Canonical type I model (*)

In this section, we show that there is a one-to-one relation between the quadratic integrate-and-fire model (5.16) and the canonical type I phase model,

$$\frac{d\phi}{dt} = [1 - \cos \phi] + \Delta I [1 + \cos \phi], \quad (5.17)$$

defined in Chapter 4; see Section 4.4.1 (Ermentrout, 1996; Ermentrout and Kopell, 1986).

Let us denote by I_θ the minimal current necessary for repetitive firing of the quadratic integrate-and-fire neuron. With a suitable shift of the voltage scale and constant current $I = I_\theta + \Delta I$ the equation of the quadratic neuron model can then be cast into the form

$$\frac{du}{dt} = u^2 + \Delta I. \quad (5.18)$$

For $\Delta I > 0$ the voltage increases until it reaches the firing threshold $\vartheta \gg 1$ where it is reset to a value $u_r \ll -1$. Note that the firing times are insensitive to the actual values

of firing threshold and reset value because the solution of Eq. (5.18) grows faster than exponentially and diverges for finite time (hyperbolic growth). The difference in the firing times for a finite threshold of, say, $\vartheta = 10$ and $\vartheta = 10000$ is thus negligible.

We want to show that the differential equation (5.18) can be transformed into the canonical phase model (5.17) by the transformation

$$u(t) = \tan\left(\frac{\phi(t)}{2}\right). \quad (5.19)$$

To do so, we take the derivative of (5.19) and use the differential equation (5.17) of the generic phase model. With the help of the trigonometric relations $d \tan x / dx = 1 / \cos^2(x)$ and $1 + \cos x = 2 \cos^2(x/2)$ we find

$$\begin{aligned} \frac{du}{dt} &= \frac{1}{\cos^2(\phi/2)} \frac{1}{2} \frac{d\phi}{dt} \\ &= \tan^2(\phi/2) + \Delta I = u^2 + \Delta I. \end{aligned} \quad (5.20)$$

Thus Eq. (5.19) with $\phi(t)$ given by (5.17) is a solution to the differential equation of the quadratic integrate-and-fire neuron. The quadratic integrate-and-fire neuron is therefore (in the limit $\vartheta \rightarrow \infty$ and $u_r \rightarrow -\infty$) equivalent to the generic type I neuron (5.17).

5.4 Summary

The standard leaky integrate-and-fire model is rather limited in scope, since it has one universal voltage threshold. Nonlinear integrate-and-fire neurons, however, can account for the fact that in real neurons the effective voltage threshold for repetitive firing is different than the voltage threshold found with short current pulses. These two voltage thresholds, which are related to the minimum of the nonlinearity $f(u)$ and to the unstable fixed point, respectively, are *intrinsic* features of nonlinear integrate-and-fire models. Once the membrane potential is above the intrinsic threshold, the upswing of the membrane potential starts. The integration is stopped at a numerical threshold θ_{reset} which is much higher and conceptually very different than the intrinsic firing threshold of the model. In fact, the exact value of the numerical threshold does not matter, since, without such a threshold, the membrane potential would go to infinity in *finite* time.

In principle, many different forms of nonlinearity are imaginable. It turns out, however, that many neurons are well described by a linear term (the “leak” term) combined with an exponential term (the “activation” term); see Fig. 5.4. Therefore, the exponential integrate-and-fire model has the “correct” nonlinearity, whereas the quadratic integrate-and-fire model is too nonlinear in the subthreshold regime and too slow in the superthreshold regime.

Both the exponential and the quadratic integrate-and-fire model show a frequency–current curve of type I. Indeed, close to the bifurcation point the two models become identical and can be mapped onto the canonical type I model.

Literature

Nonlinear generalizations of the one-dimensional equation of the leaky integrate-and-fire model can be found in the paper by Abbott and van Vreeswijk (1993). While the form of the nonlinearity was left open at that time, analytical methods from bifurcation theory suggested that there was a canonical one-dimensional model which describes the saddle-node-onto-limit-cycle bifurcation of type I models. This is called the canonical type I model or Theta model or Ermentrout–Kopell model (Ermentrout and Kopell, 1986; Ermentrout, 1996). While the quadratic nonlinearity in the voltage appeared in many early papers on bifurcations and type I models (Ermentrout, 1996; Ermentrout and Kopell, 1986; Strogatz, 1994; Hoppensteadt and Izhikevich, 1997) the active use of the quadratic integrate-and-fire model for simulations seems to have been started by Latham et al. in 2000 and later popularized by Izhikevich (2007b).

Based on biophysical and mathematical arguments, the exponential integrate-and-fire model was introduced in 2003 by Fourcaud-Trocme, Hansel, Vreeswijk and Brunel. While the quadratic integrate-and-fire model is the canonically correct type I model close to the bifurcation point, i.e., at the transition to repetitive firing, there is no fundamental reason why the quadratic nonlinearity should also be correct further away from the threshold, and it was unclear at that time what the nonlinearity of real neurons would look like. The issue was settled by the work of Badel *et al.* (2008a,b) who designed an experimental method to measure the nonlinearity directly in experiments. The nonlinearity found in experiments is extremely well matched by the exponential integrate-and-fire model.

The link between ion channel activation or inactivation in conductance-based neuron models and the parameters of an exponential integrate-and-fire model with refractoriness (Badel *et al.*, 2008a,b) is discussed in the overview paper by Platkiewicz and Brette (2010).

We shall see in the next chapter that the single-variable exponential integrate-and-fire model as it stands is not sufficient to account for the wide variety of neuronal firing patterns, but needs to be complemented by a second variable to account for slow processes such as adaptation – and this leads eventually to the adaptive exponential integrate-and-fire model.

Exercises

1. **Quadratic vs. exponential integrate-and-fire.** For a comparison of the two models, take a look at Fig. 5.8b and answer the following questions:
 - (a) Show for the exponential integrate-and-fire model that the minimum of the nonlinearity $f(u)$ occurs at $u = \vartheta_{\text{rh}}$. Calculate the curvature $d^2/du^2 f(u)$ at $u = \vartheta_{\text{rh}}$.
 - (b) Find parameters of the quadratic integrate-and-fire model so that it matches the location and curvature of the exponential model in (a).
 - (c) Suppose that the value of the numerical threshold is $\theta_{\text{reset}} = \vartheta_{\text{rh}} + 2\Delta_T$. When the threshold

is reached the membrane potential is reset to $u_r = \vartheta_{\text{rh}} - 2\Delta_T$. Sketch qualitatively the trajectory $u(t)$ for both neuron models in the repetitive firing regime. Pay particular attention to the following questions: (i) For $u > \vartheta_{\text{rh}}$ which of the two trajectories rises more rapidly towards the numerical threshold? (ii) For $u = \vartheta_{\text{rh}}$, do both trajectories have the same speed of rise du/dt or a different one? (iii) For $u < \vartheta_{\text{rh}}$, which of the two trajectories rises more rapidly? (iv) Should your drawing of the trajectories follow any symmetry rules? Compare your results with Fig. 5.9.

2. **Zero-curvature and rheobase threshold.** Experimenters sometimes determine the threshold voltage for spike initiation by searching for the zero-curvature point in the voltage trajectory, just before the upswing of the action potential. Show for a general nonlinear integrate-and-fire model that the zero-curvature point is equivalent to the rheobase threshold ϑ_{rh} . Hints: (i) Minimal curvature means that the voltage trajectory passes through a point $d^2u/dt^2 = 0$. (ii) Note that the slope of the voltage trajectory du/dt is given by the function $f(u)$. (iii) Recall that the minimum of f is taken at $u = \vartheta_{\text{rh}}$.
3. **Exponential integrate-and-fire and sodium activation.** To derive the exponential integrate-and-fire model from a Hodgkin–Huxley model with multiple channels, follow the procedure indicated in Section 5.2.2 and perform the following steps.

(a) Show that N linear currents can always be rewritten as one effective leak current $\sum_k g_k (u - E_k) = g^{\text{eff}} (u - E^{\text{eff}})$. Determine the effective conductance g^{eff} and the effective reversal potential E^{eff} .

(b) Assume that the sodium activation is rapid and approaches an equilibrium value $m_0(u) = 1 / \{1 + \exp[-\beta(u - \theta_{\text{act}})]\} = 0.5 \{1 + \tanh[-\beta(u - \theta_{\text{act}})/2]\}$ where θ_{act} is the activation threshold of the sodium channel and β the sharpness of the threshold. Using a Taylor expansion, show that for $u < \theta_{\text{act}} - \beta^{-1}$ the activation function can be approximated by an exponential $m_0(u) = \exp[\beta(u - \theta_{\text{act}})]$.

(c) Assume that $u < \theta_{\text{act}} - \beta^{-1} < E_{\text{Na}}$ and show that the sodium current

$$I_{\text{Na}} = g_{\text{Na}} [m_0(u)]^3 h_{\text{rest}} (u - E_{\text{Na}}) \quad (5.21)$$

gives rise to the exponential term.

(d) Using the steps (a) – (c), map (5.15) to the exponential integrate-and-fire model

$$\frac{du}{dt} = \tilde{f}(u) = -\frac{u - u_{\text{rest}}}{\tau} + \frac{\Delta_T}{\tau} \exp\left(\frac{u - \vartheta_{\text{rh}}}{\Delta_T}\right). \quad (5.22)$$

Determine the parameters u_{rest} , τ and Δ_T .

4. **Refractory exponential integrate-and-fire model and sodium inactivation.** In the previous exercise, we have assumed that $h = h_{\text{rest}}$ is constant throughout the spiking process. Repeat the steps of the previous calculation, but set $h(t) = h_{\text{rest}} + x(t)$ and show that the sodium inactivation dynamics leads to an increase in the firing threshold a few milliseconds after the spike.

Hints. (i) Linearize the dynamics of gating variable h in the Hodgkin–Huxley model around $h = h_{\text{rest}}$ so as to derive $dx/dt = -x/\tau_0$. (ii) Assume that during each spike, the inactivation variable h increases by a fixed amount Δh .

5. **Quadratic integrate-and-fire model.**

Consider the dimensionless quadratic integrate-and-fire model

$$\frac{d}{dt}u = (u - u_{\text{rest}})(u - u_c) + I, \quad (5.23)$$

with $u_{\text{rest}} = -1$ and $u_c = 1$ and $I = 0$.

(a) Suppose that a trajectory starts at time $t = 0$ at $-\infty$. How long does it take to get close to the resting state and reach the value $u = -1 - \varepsilon$ where $\varepsilon \ll 1$?

(b) Suppose that a trajectory is initialized at $u(0) = 1 + \varepsilon$, where $\varepsilon \ll 1$. How long does it take to reach $u = \infty$?

(c) Initialize as in (b) but stop the integration at $u = \theta_{\text{reset}}$. How long does the trajectory take to reach the reset threshold? Is the difference between (b) and (c) important?